

This is the author-created version of the following work:

**Haig, Jordahna, Ascough, Philippa, Wurster, Christopher M., and Bird, Michael I. (2020) *A rapid throughput technique to isolate pyrogenic carbon by hydrogen pyrolysis for stable isotope and radiocarbon analysis*. *Rapid Communications in Mass Spectrometry*, 34 (10) .**

Access to this file is available from:

<https://researchonline.jcu.edu.au/67133/>

© 2020 John Wiley & Sons, Ltd.

Please refer to the original source for the final version of this work:

<http://doi.org/10.1002/rcm.8737>

1 **A rapid throughput technique to isolate pyrogenic carbon by hydrogen pyrolysis for**  
2 **stable isotope and radiocarbon analysis**

3 Jordahna Haig<sup>1</sup>, Philippa L. Ascough<sup>2</sup>, Christopher M. Wurster<sup>1</sup>, Michael I. Bird<sup>1</sup>

4 <sup>1</sup>College of Science and Engineering, ARC Centre of Excellence of Australian Biodiversity  
5 and Heritage and Centre for Tropical Environmental and Sustainability Science, James Cook  
6 University, Cairns, QLD 4870, Australia

7 <sup>2</sup>NERC Radiocarbon Facility, SUERC, Scottish Enterprise Technology Park, Rankine  
8 Avenue, East Kilbride, G75 0QF, UK

9

10 Keywords: Radiocarbon pretreatment; pyrogenic carbon; hydrogen pyrolysis; charcoal

11

12 **Abstract**

13 **RATIONALE:** Rapid, reliable isolation of Pyrogenic Carbon (PyC; char, soot, black carbon;  
14 biochar) for determination of stable carbon isotope ( $\delta^{13}\text{C}$ ) composition and radiocarbon ( $^{14}\text{C}$ )  
15 dating is needed across multiple fields of research in geoscience, environmental science and  
16 archaeology. Many current techniques do not provide reliable isolation from contaminating  
17 organics and/or are relatively time consuming to employ. Hydrogen pyrolysis (HyPy) does  
18 provide reliable isolation of PyC but the current methodology is time consuming.

19 **METHODS:** We explored the potential for subjecting multiple samples to HyPy analysis by  
20 placing up to nine individual samples in custom designed borosilicate sample vessels in a  
21 single reactor run. We tested for cross contamination between samples in the same run using  
22 materials with highly divergent radiocarbon activities (~0.04 to 116.3 pMC),  $\delta^{13}\text{C}$  values (-

23 11.9 to -26.5‰) and labile carbon content. We determined  $^{14}\text{C}/^{13}\text{C}$  by accelerator mass  
24 spectrometry and  $\delta^{13}\text{C}$  values by elemental analyser coupled to continuous flow isotope ratio  
25 mass spectrometer.

26 **RESULTS:** Very small but measurable transfer between samples of highly divergent isotope  
27 composition was detectable. Where samples are of broadly similar composition, this cross  
28 contamination is considered negligible with respect to measurement uncertainty. Where  
29 samples are of divergent composition, it was found that placing a sample vessel loaded with  
30 silica mesh adsorbent between samples eliminated measurable cross-contamination in all  
31 cases for both  $^{14}\text{C}/^{13}\text{C}$  and  $\delta^{13}\text{C}$  values.

32 **CONCLUSION:** It is possible to subject up to seven samples to HyPy in the same reactor  
33 run for determination of radiocarbon content and  $\delta^{13}\text{C}$  value without diminishing the  
34 precision or accuracy of the results. This approach enables an increase in sample throughput  
35 of 300-600%. HyPy process background values are consistently lower than the nominal  
36 laboratory process background for quartz tube combustion in the NERC Radiocarbon  
37 Laboratory, indicating that HyPy may also be advantageous as a relatively ‘clean’  
38 radiocarbon pretreatment method.

## 39 1. Introduction

40 Pyrogenic carbon (PyC, also known as char, black carbon, biochar) is derived from the  
41 incomplete combustion (pyrolysis) of organic matter during natural fires, the purposeful  
42 pyrolysis of biomass to create ‘biochar’, or via fossil fuel combustion [1,2]. PyC is a  
43 ubiquitous component of carbon in soils, sediments, atmospheric particulates, fresh and  
44 marine waters, in both dissolved and/or particulate (microscopic and macroscopic) forms.

45 PyC is important as a poorly understood, slow-cycling component of the global carbon  
46 cycle, that is now known to comprise a significant, but as yet unquantified, pool that contains  
47 some of the most recalcitrant organic carbon on Earth [3,4]. In the form of biochar, PyC also  
48 has the potential to sequester significant amounts of carbon over time periods far exceeding  
49 that of biomass, therefore offsetting at least a proportion of current anthropogenic CO<sub>2</sub>  
50 emissions [5]. PyC is also useful as a form of recalcitrant carbon that can provide a valuable  
51 palaeoenvironmental proxy through its stable isotope composition [6]. It is one of the most  
52 common materials (as ‘charcoal’) used for construction of radiocarbon chronologies in  
53 support of archaeological and Quaternary environmental studies.

54 Quantification and isolation of PyC has long proven problematic. This is because PyC  
55 represents a continuum of complex molecular components with differing chemical and  
56 spectroscopic properties. Each method targets a particular ‘window’ along this continuum,  
57 meaning the ‘PyC’ isolated by two differing methods can be chemically quite distinct. Thus,  
58 while many techniques have been developed to analyse PyC in a range of environmental  
59 matrices, these techniques produce widely divergent results for the same samples, the same  
60 technique has produced divergent results across different laboratories and some techniques  
61 are not broadly applicable across the range of matrices that can contain PyC [7]. The key  
62 difficulty however, is that many methods rely on an operational definition of PyC in order to  
63 achieve isolation. This often requires that what remains after the process must, by definition,  
64 be PyC, and that quantification relies upon a single parameter, such as weight loss during  
65 processing. Problems arise if non-PyC material is not removed e.g. due to hydrophobic  
66 protection of plant waxes in aqueous solutions [8], or if PyC is formed *de novo* during  
67 oxidative reactions [9]. Procedures isolating PyC on a secure chemically-defined basis, are  
68 therefore preferable.

69 Hydrogen pyrolysis (HyPy) was originally used as a method for the efficient conversion of  
70 macromolecular organic matter to dichloromethane soluble oils with conversions near 100%  
71 possible using high hydrogen pressures (>10 MPa) at high temperature [10]. During these  
72 experiments, it was found that in some cases substantial amounts of highly aromatic  
73 macromolecular carbon remained in the residues, attributed to PyC [11].

74 The possibility that HyPy could be used to quantify PyC was first discussed by Ascough et  
75 al [12,13], who developed a hydrogen pyrolysis procedure specific to eliminating labile  
76 components and leaving only polyaromatic carbon in the residue. Meredith et al [14]  
77 demonstrated that HyPy yielded results within the range of other techniques for PyC in a  
78 range of matrices using the black carbon ring trial samples of Hammes et al [7]. Meredith et  
79 al [14] also demonstrated that HyPy was able to remove potentially interfering non-pyrogenic  
80 materials with the exception of anthracite, and that the component isolated by HyPy is  
81 chemically highly consistent, being polyaromatic carbon with a ring size greater than 7  
82 (coronene). Smaller pyrogenic polyaromatic molecules can be collected by cryogenic  
83 trapping downstream of the HyPy reactor for separate quantification if required [15-17].  
84 More recent work has demonstrated the utility of HyPy analysis across a range of  
85 environmental matrices, for simple quantification [18-20] with good reproducibility within  
86 and between laboratories [21], as well for stable isotope analysis [6,22,23] and radiocarbon  
87 dating [12,13,24,25].

88 While the advantages of HyPy for the isolation and quantification of a well-defined  
89 component of PyC have now been clearly demonstrated, the technique remains relatively  
90 slow. The instrument reactor conventionally accommodates one sample at a time and a single  
91 run takes approximately 43 minutes. While the technique is not more time consuming than  
92 many other competing techniques, the current throughput limits the scale of projects that can  
93 be undertaken. At the same time, research interest in PyC is growing rapidly, particularly for

94 carbon-cycle science applications. For example, measuring PyC abundance and turnover  
95 times by  $^{14}\text{C}$ , which by their nature require high-volume throughput. The general need to  
96 improve throughput is now driving modifications to other established techniques such as  
97 BPCA analysis [26].

98 Here we report on the results of experiments designed to test whether multiple samples can  
99 be run simultaneously in a single HyPy reactor for accelerated throughput and efficiency,  
100 without either cross contaminating the samples or degrading the accuracy or precision of  
101 individual stable isotope and radiocarbon analyses.

## 102 **2. Materials and Methods**

### 103 2.1 Samples

104 The samples for this study were chosen to provide the largest possible contrast in lability  
105 of material (i.e. degree of aromaticity), and in carbon isotope ( $\delta^{13}\text{C}$  and  $^{14}\text{C}$ ) composition.  
106 Five matrixes were chosen for experiments designed to test the degree to which combining  
107 multiple samples with divergent characteristics in a single reactor run effected the measured  
108 PyC abundance,  $\delta^{13}\text{C}$  and  $^{14}\text{C}$  measurements of individual samples in the same reactor (see  
109 Table 1.). Throughout this manuscript, error is reported as  $2\sigma$ .

110 **Three** materials of known radiocarbon content were chosen for experiments designed to  
111 test, 1) the  $^{14}\text{C}$  background of the HyPy process itself, and 2) the degree of inter-sample  
112 transfer of carbon when combining multiple samples with different  $^{14}\text{C}$  content in a single  
113 HyPy run:

114 (i) *TIRI barley mash (TBM)*: This standard originates from the Third International  
115 Radiocarbon Intercomparison [27]. It is composed of lignocellulosic biomass, known to be  
116 entirely labile during HyPy. The consensus value for TBM is  $116.35 \pm 0.016$  pMC. TBM was  
117 used as a source of excess labile C from a sample in HyPy, which thus had the potential to be

118 transferred to other samples in the same HyPy reactor. The relatively high  $^{14}\text{C}$  content of  
119 TBM makes it possible to detect even small quantities of cross-contamination, when used  
120 with a contrasting RCD (radiocarbon dead) material (below).

121 (ii) *Anthracite*: This is a NERC Radiocarbon Facility in-house process standard anthracite  
122 [28]. It is a highly aromatic material, and anthracite coal is known to be resistant to HyPy  
123 [14]. This material is 'radiocarbon-dead', being much greater than 50,000 years in age, and is  
124 in use as a process background material for radiocarbon analyses. For the quartz tube  
125 combustion method of  $\text{CO}_2$  production (the process applied in this study), the long-term  
126 average background value at the NERC Radiocarbon laboratory is  $0.17 \pm 0.02$  pMC. The  
127 anthracite standard was used to identify whether the HyPy  $^{14}\text{C}$  background was  
128 commensurate with this value before, during, and after the experiments described below, and  
129 to provide confidence that any observed variation in  $^{14}\text{C}$  during multiple simultaneous HyPy  
130 runs can be ascribed to a specific process (i.e. transfer of carbon between sample vessels  
131 within the reactor for this specific experiment), and not an inherent feature of the method  
132 itself.

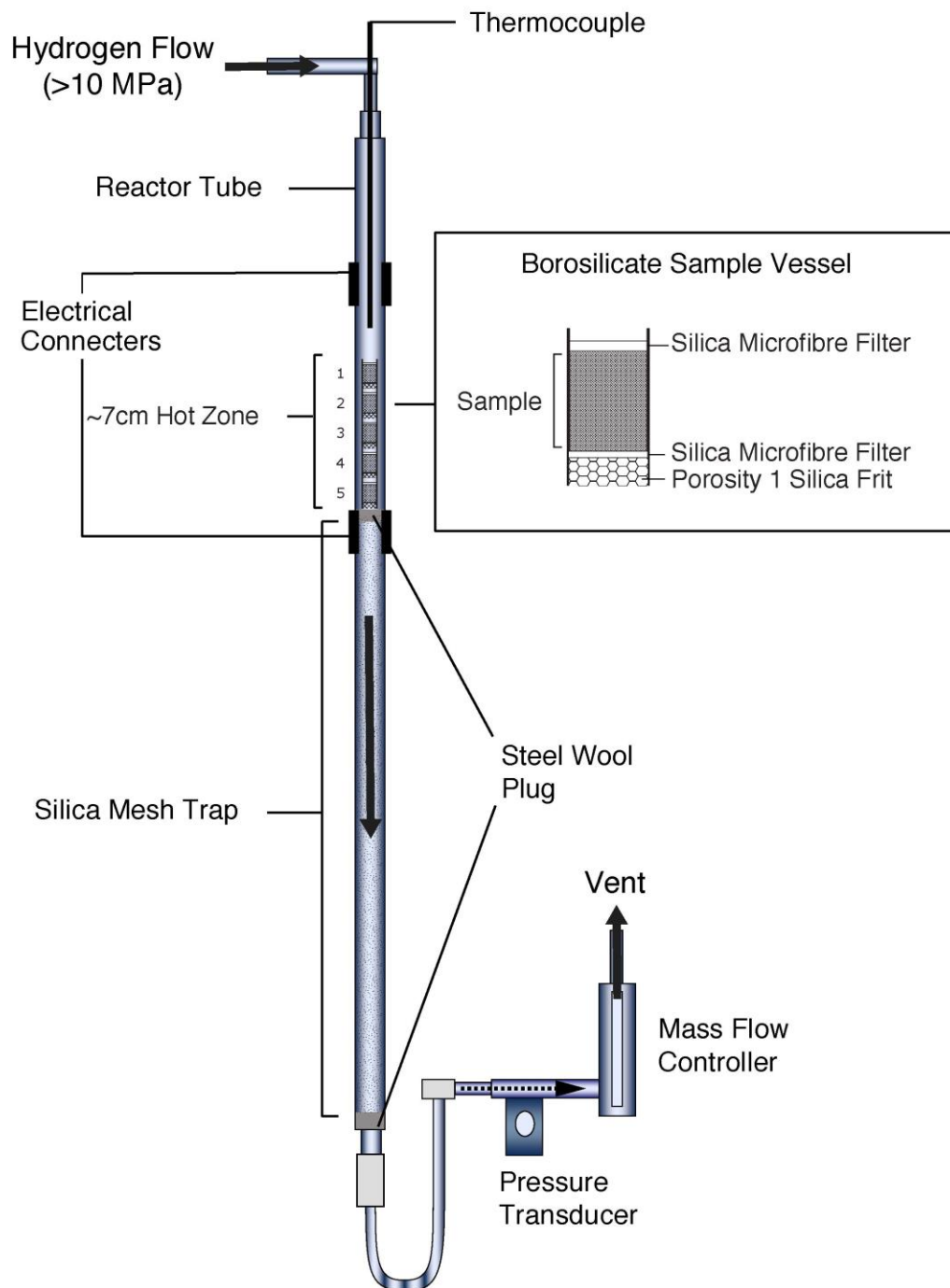
133 (iii) *RDC*: This is a radiocarbon-dead charcoal produced experimentally from a log of  
134 Miocene age and previously characterized by Bird et al [29]. It is a material resistant to  
135 conversion during HyPy, with a radiocarbon activity equivalent to  $0.04 \pm 0.02$  pMC. This  
136 material is also highly aromatic, similar to the anthracite coal standard, but was included as it  
137 represents a more typical form of natural PyC (i.e. the product of biomass that has been  
138 thermally altered during fire). During the experiments below, RDC was used to represent  
139 material into which the introduction of cross-contamination (from TBM) during HyPy could  
140 be monitored.

141 2.2 Hydrogen pyrolysis

142 Hydrogen pyrolysis has been described in detail in a number of publications [10,30,12,14].  
143 Briefly, 25-100 mg aliquots of each sample were loaded with a Mo catalyst using an  
144 aqueous/methanol (1:1) solution of ammonium dioxodithiomolybdate  $[(\text{NH}_4)_2\text{MoO}_2\text{S}_2]$ .  
145 Catalyst weight was ~10% sample weight for all samples to give a nominal loading of ~1%  
146 Mo. Catalyst loaded samples were then lyophilized and weighed aliquots of each sample  
147 were loaded into small bespoke borosilicate sample vessels of 7 mm outer diameter, 1 mm  
148 wall thickness and 10 mm (small) or 15 mm (large) overall length. The base of each sample  
149 vessel was fitted with a porosity #1 silica frit to allow gas throughflow (manufactured by  
150 Robson Scientific, Sawbridgeworth, UK). Small glass microfiber filters ~5mm in diameter  
151 were used to line the bottom of the vessel and plug the top of the vessel to keep the sample in  
152 place. These are hole-punched using a cork borer from standard Whatman 0.45  $\mu\text{m}$  glass  
153 microfiber filters.

154 In order to facilitate higher throughput (i.e. >1 sample per reaction) the HyPy reactor setup  
155 was modified from that outlined in Ascough et al [12]. In this study, the 1/4" silica trap has  
156 been removed and the standard 254mm 9/16" reactor has been replaced with a 475mm nipple  
157 (see Fig. 1). The upper 196mm of the nipple now functions as the reactor while the bottom  
158 279mm is filled with silica mesh and used as a trap to collect the products of the reaction (i.e.  
159 the labile carbon fraction). This larger trap does not require cleaning for upwards of 45  
160 reactions.

161 Multiple samples (4-9) were loaded one above the other into the HyPy reactor as per the  
162 experimental design outlined in Figure 2. After sample loading, the reactor was pressurized  
163 with hydrogen to 15 MPa with a flow rate of 5 L  $\text{min}^{-1}$ , then heated using a pre-programmed  
164 temperature profile. We used the recommended temperature program previously optimized  
165 for PyC quantification where samples are initially heated at a rate of 300°C  $\text{min}^{-1}$  to 250°C,  
166 then at a rate of 8°C  $\text{min}^{-1}$  until the final hold temperature of 550°C for 5min [12,14].



167

168 **Figure 1.** *Hydrolysis reactor schematic showing placement and design of the*  
 169 *borosilicate sample vessels, steel wool placeholder, silica trap and direction of Hydrogen*  
 170 *flow.*

171

172

### 173 2.3 Carbon abundance and stable isotope composition

174 Carbon abundances and isotope compositions of all samples were determined using a  
175 Costech Elemental Analyzer (Costech Analytical Technologies Inc., Valencia, CA,  
176 USA) fitted with a zero-blank autosampler coupled via a ConFloIV (Thermo Fisher  
177 Scientific, Waltham, MA, USA) to a ThermoFinnigan DeltaV<sup>PLUS</sup> using Continuous-Flow  
178 Isotope Ratio Mass Spectrometry (EA-IRMS) at the Advanced Analytical Unit at James  
179 Cook University, Cairns. Stable isotope results are reported as per mil (‰) deviations from  
180 the VPDB reference standard scale for  $\delta^{13}\text{C}$  values. Precisions ( $2\sigma$ ) on internal standards were  
181 better than  $\pm 0.2$  ‰. Because the catalyst undergoes ( $\sim 25\%$ ) weight loss during HyPy, the  
182 abundance of residual carbon in the sample after hydrogen pyrolysis is determined as the  
183 mass of carbon after treatment relative to the mass of carbon loaded and the results reported  
184 as the residual carbon present in the sample ( $C_{\text{R}}$ – residual carbon not removable by HyPy).  
185 Reproducibility is considered to be 2% of the value, based on repeated analyses [31].

### 186 2.4 Radiocarbon measurement

187 HyPy residues were converted to  $\text{CO}_2$  by combustion in sealed quartz tubes, and the  
188 evolved gas was cryogenically purified and converted to graphite for analysis using Fe/Zn  
189 reduction [32]. Sample  $^{14}\text{C}/^{13}\text{C}$  ratios were measured by Accelerator Mass Spectrometry [29]  
190 at the Scottish Universities Environmental Research Centre. Measured  $^{14}\text{C}/^{13}\text{C}$  ratios were  
191 normalized to a  $\delta^{13}\text{C}$  value of  $-25$ ‰ and expressed as % modern carbon (pMC) according to  
192 Stuiver and Polach [33].

### 193 2.5 Experimental Design

194 The experimental design is given in Figure 2, it comprises four sets of experiments using  
195 the materials described in table 1.

196 (i) *Experiment 1:* The purpose of this experiment was to determine the location of the  
197 reactor ‘hot zone’ i.e. the region where the temperature is consistent and hydrogen pyrolysis  
198 is effective and reproducible. This zone defines the maximum number of samples that can be  
199 run simultaneously using the modified reactor setup. Initially, 9 small (10 mm long) sample  
200 vessels containing ~100mg of a reference material (BCM) were run in quadruplicate. This  
201 experiment was repeated with 6 large (15 mm long) sample vessels of a composite soil  
202 control sample (AGR), also run in quadruplicate.

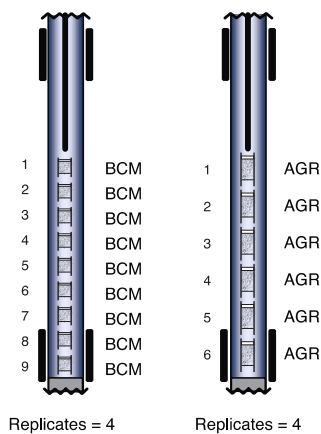
203 (ii) *Experiment 2:* In this experiment, (fig 2a), ~30mg of anthracite was first used to  
204 determine the HyPy <sup>14</sup>C background for the radiocarbon experiments. Measurements of  
205 anthracite were also performed before and after a HyPy run, to test for any sequential changes  
206 in the HyPy instrument <sup>14</sup>C background. Two RDC samples were used as controls. In  
207 experiment 2a, ~100mg (replicate 1) or ~50mg (replicate 2) of TBM was placed vertically  
208 above three RDC samples in the same reactor. The TIRI standard and three RDC samples  
209 were all contained in the same HyPy reactor run to test whether labile carbon is transferred  
210 from the sample above to the samples below, in the direction of hydrogen flow, manifest in a  
211 measurable increase in radiocarbon in the RDC samples. This experiment was repeated in  
212 experiment 2b, with the addition of a sample vessel filled with 70-200µm silica mesh  
213 between the ~50mg of TBM and RDC samples, replicated twice.

214 *Experiment 3:* The purpose of this experiment was to quantify the amount of labile TOC  
215 is transferred ‘downstream’ from one vessel to another over the course of a single reactor run.  
216 To do this, 2-10mg of carbon (in the form of Sugarcane Leaves or BCM) was placed in a  
217 sample vessel above a series of four silica mesh spacers, with or without an empty sample  
218 vessel (acting as a spacer) at position 2. The silica mesh was analysed for C abundance by  
219 Costech elemental analyser immediately following the HyPy. In addition, a background silica

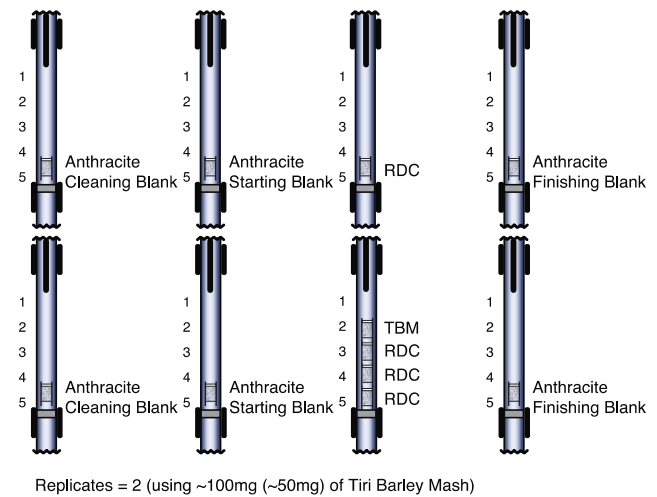
220 mesh carbon abundance was determined by successive HyPy runs comprising exclusively  
 221 silica mesh spacers.

222 *Experiment 4:* The purpose of this experiment was to test the degree to which labile  
 223 carbon released from one sample during a HyPy run, is transferred to another ‘downstream’  
 224 sample within the HyPy reactor. In this experiment an inhouse reference of labile C<sub>3</sub>(C<sub>4</sub>)  
 225 material, C<sub>3</sub> rainforest leaves (or C<sub>4</sub> sugarcane leaves) was placed in a sample vessel above a  
 226 vessel loaded with a C<sub>4</sub> (or C<sub>3</sub>) soil sample containing PyC of known abundance and stable  
 227 isotope composition, both with and without a silica mesh spacer at position 2 (fig 2d). This  
 228 experiment was repeated in quadruplicate.

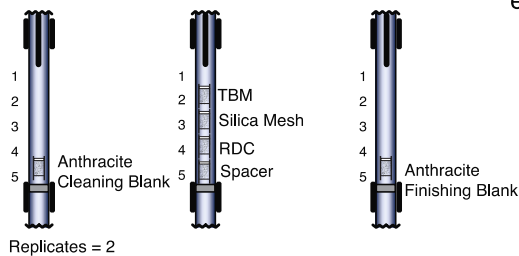
a) Experiment 1: Position experiment



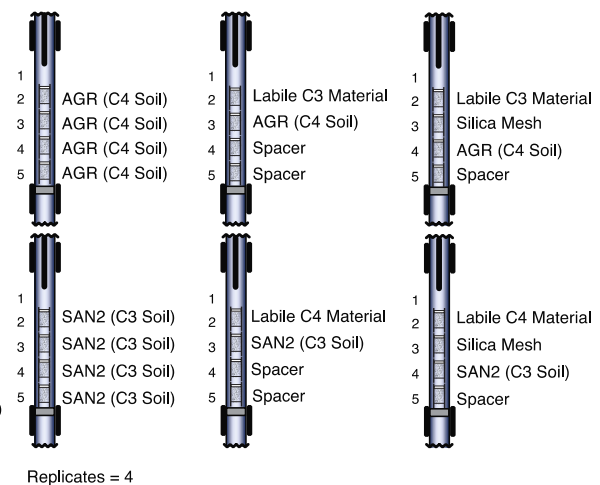
b) Experiment 2a: Radiocarbon Experiment a



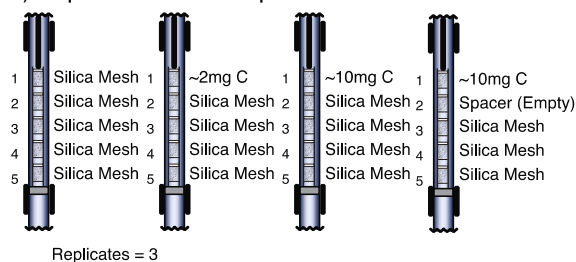
c) Experiment 2b: Radiocarbon Experiment b



e) Experiment 4: δ<sup>13</sup>C Experiment



d) Experiment 3: Si Experiment



230 **Figure 2.** *Experimental design, showing the position and contents of the sample vessels in*  
231 *each HyPy experiment run, the number of replicates and the order of runs. A) position*  
232 *experiment to determine the ideal number of samples per run and the location of the ‘hot*  
233 *zone’ within the reactor; B) radiocarbon experiment A, to determine if running multiple*  
234 *samples simultaneously leads to <sup>14</sup>C contamination of samples below; C) radiocarbon*  
235 *experiment B, to determine if adding silica mesh spacers between samples reduces <sup>14</sup>C*  
236 *contamination of the sample below; D) silica mesh experiment to quantify the transfer of*  
237 *labile C down the profile, with or without an empty sample vessel (spacer) E) Replication of*  
238 *the previous experiments to test whether typical C<sub>3</sub> (C<sub>4</sub>) soil samples are contaminated by*  
239 *labile C<sub>4</sub> (C<sub>3</sub>) material from the vessel directly above, and if a silica mesh spacer resolves*  
240 *this.*

241

242 Pairwise multiple comparison tests were used in experiment 1 to determine whether PyC%  
243 was influenced by position within the HyPy reactor, and to identify the area within the reactor  
244 in which the variability was least (i.e. the ‘hot zone’) and thus the ideal positioning of the  
245 steel wool plug that holds all the vessels in place in the reactor (Figure 1). Pairwise multiple  
246 comparison tests were also used in experiment 4 to determine whether the amount of labile  
247 carbon above a sample impacts the  $\delta^{13}\text{C}$  value of PyC in a sample downstream.

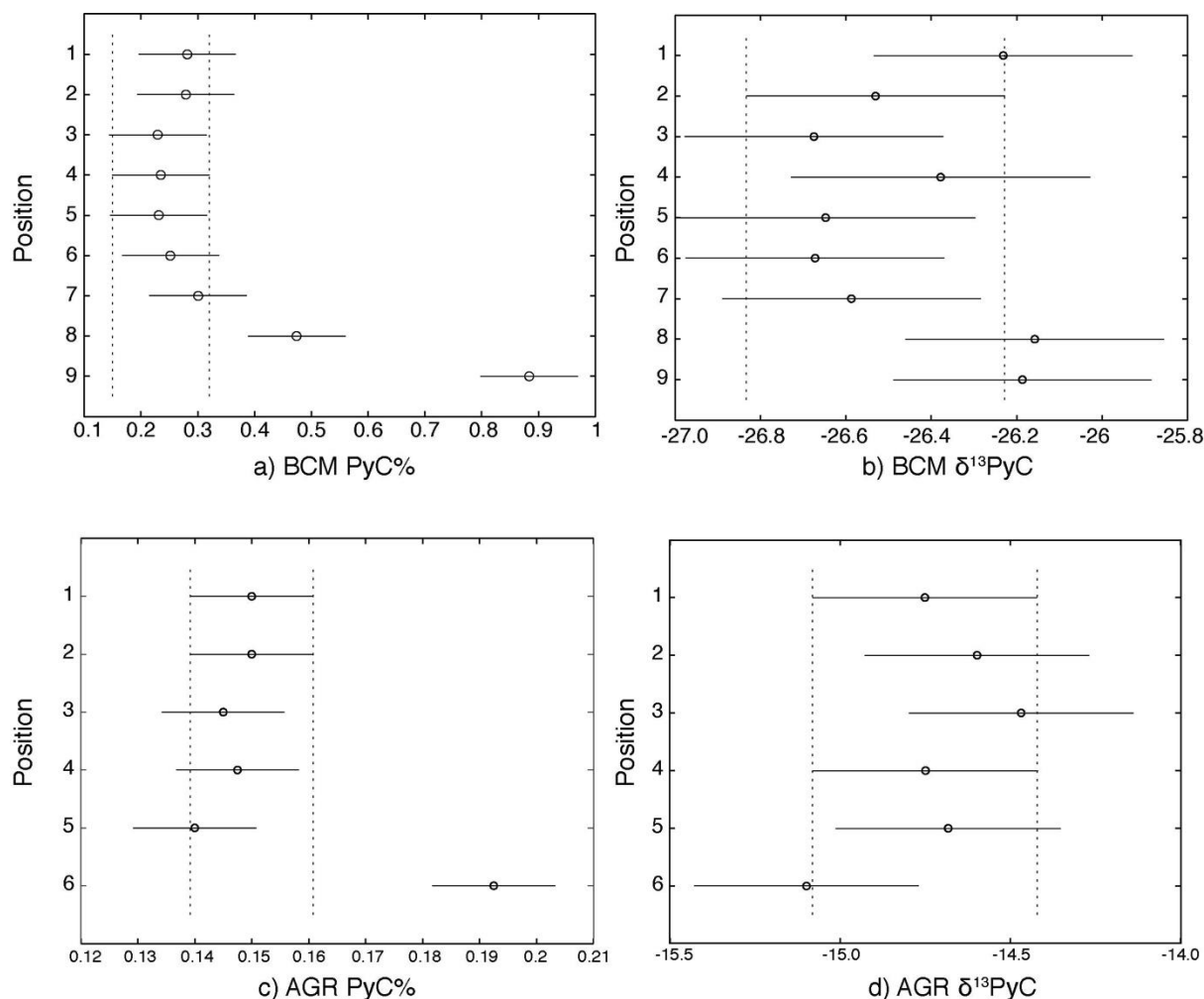
### 248 **3. Results and Discussion**

#### 249 3.1 Experiment 1: ‘hot zone’ delimitation

250 In conventional HyPy, samples are processed individually in a 43 minute HyPy run  
251 [12,14]. To determine the feasibility of running multiple samples simultaneously, multiples of  
252 9 small sample vessels (10 mm; n = 26 total) or 5 large sample vessels (15 mm; n = 20 total)  
253 stacked on top of each other, were run within the same reactor in quadruplicate runs to

254 determine the maximum number of samples that can be run in tandem without compromising  
255 precision. Across all positions PyC ranged from 0.2 - 1.1% (0.1 - 0.2%) and  $\delta^{13}\text{PyC}$  ranged  
256 from -26.3 to -26.6‰ (-15.4 to -14.2‰) for the experiments based on BCM (AGR). The  
257 summary statistics are given in table 2.

258 Comparison of the results by position in the reactor (fig 3a) shows that results from the 10mm  
259 vessels (BCM) in position 8 and 9 do not belong to the same population as samples 1-7,  
260 indicating that the 'hot zone' is within ~7cm of the thermocouple tip in the reactor ( $\mu = 0.3$   
261  $\pm 0.08\%$ ,  $-26.5 \pm 0.6\%$ ), below this reproducibility is diminished. A repeat of the same  
262 experiment using 15mm vessels (fig 3c: AGR) confirms the ~7cm hot zone as there is no  
263 statistical difference in PyC% between samples in positions 1-5 i.e. within ~7.5cm of the  
264 thermocouple ( $\mu = 0.2 \pm 0.01\%$ ,  $-14.7 \pm 0.3\%$ ). Position affects PyC% to a greater extent than  
265  $\delta^{13}\text{PyC}$  (fig 3b and 3d) as there is no statistical difference between any position when using  
266 either small or large vessels providing an error ( $2\sigma$ ) of 0.6‰ and 0.3‰ is acceptable. This  
267 confirms that multiples of 7 (small 10 mm vessels) or 5 (large 15 mm vessels) samples can be  
268 accurately run together within a single 45 minute HyPy run, with a precision better than  
269 0.08% PyC and 0.6‰  $\delta^{13}\text{PyC}$ , equating to a 400-600% increase in throughput compared to  
270 the conventional 'single sample per run' method.



271

272 **Figure 3.** Pairwise multicomparison plot showing test estimates i.e. group mean  $\mu$  (circles),  
 273 and comparison intervals  $\alpha$  (lines) for 10mm sample vessels of BCM PyC% (A) and  $\delta^{13}\text{PyC}$   
 274 (B); and 15mm sample vessels of AGR composite soil PyC% (C) and  $\delta^{13}\text{PyC}$  (D).

275 3.2 Experiment 2a: Radiocarbon pretreatment background

276 HyPy has already been successfully applied as a rapid pretreatment method for isolating  
 277 and purifying PyC for  $^{14}\text{C}$  measurements [12,13,24,25]. Experiment 1 confirmed that it is  
 278 statistically acceptable to process up to 5 large samples in tandem for PyC quantification by  
 279 HyPy. In experiment 2, we assess the potential for pre-treating multiple samples  
 280 simultaneously when radiocarbon measurement of these samples is also required. To  
 281 determine the appropriate HyPy radiocarbon pretreatment background, a series of anthracite  
 282 cleaning, and finishing blanks were run in isolation before and after each experiment.

283 Combining all anthracite runs indicates a HyPy background value of 0.13 pMC ( $\mu = 0.10$ ,  $2\sigma$   
284  $= 0.03$ ,  $n = 11$ ). This is significantly less than the standard internal NERC Radiocarbon  
285 Laboratory quartz tube process background value of  $0.17 \pm 0.02$  pMC. The anthracite finishing  
286 blanks run immediately after each experiment were indistinguishable from the lab process  
287 background ( $\mu = 0.10$ ,  $\sigma = 0.04$ ), meaning there is no detectable additional  $^{14}\text{C}$  added by the  
288 HyPy process above that of the quartz tube combustion when compared to standard process  
289 background values.

290 These results indicate that normal cleaning between HyPy runs (i.e. manual rinsing of the  
291 reactor with dichloromethane, followed by drying of the reactor and complete removal of  
292 dichloromethane during the warm-up phase of HyPy treatment, is sufficient to preserve  
293 appropriate  $^{14}\text{C}$  background values. Indeed, the measured HyPy process background values  
294 were consistently lower than the nominal laboratory process background for the quartz tube  
295 method of combustion, indicating that the HyPy process may be a particularly ‘clean’  
296 pretreatment for samples in comparison with other methods applied to PyC (as charcoal),  
297 such as the Acid-Base-Acid processing protocol. This result is promising and warrants further  
298 investigation.

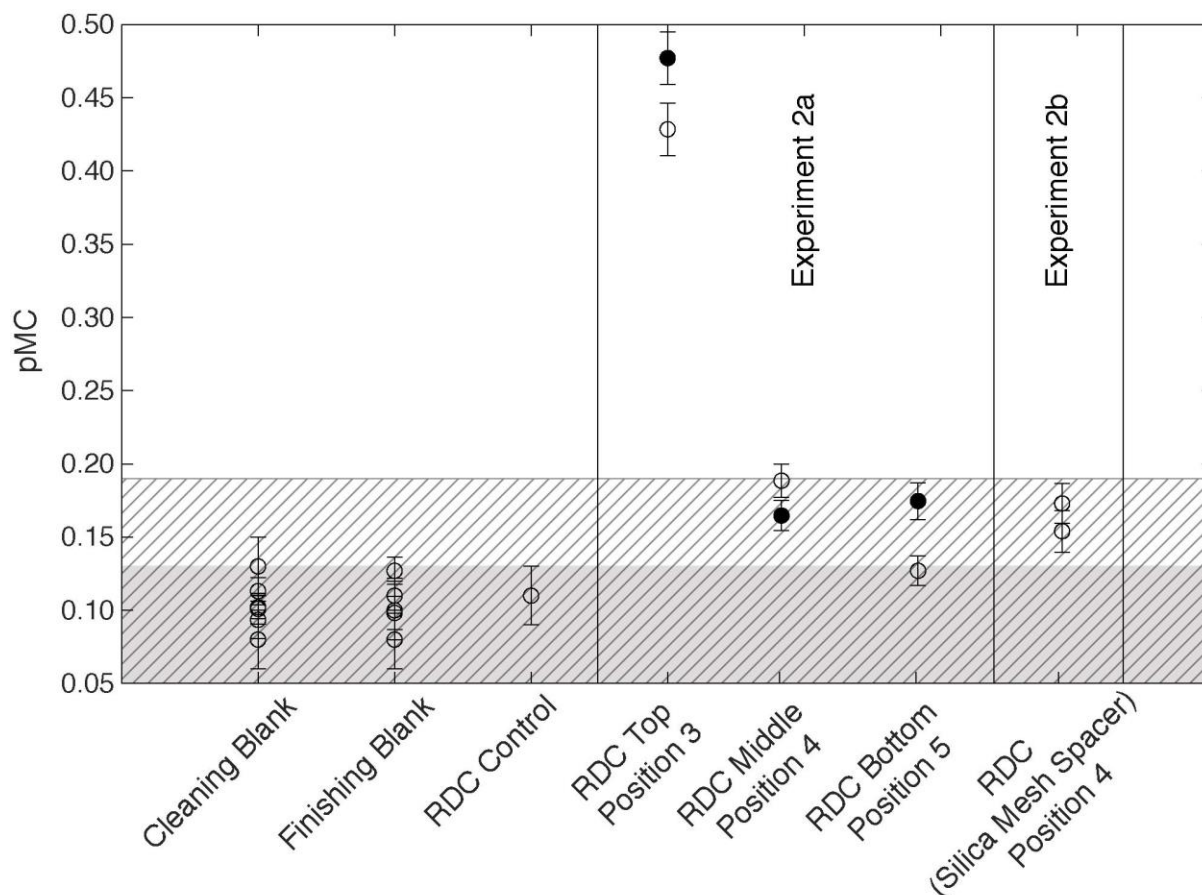
### 299 3.3 Experiment 2b: Assessment of downstream contamination potential by radiocarbon

300 To assess the potential for transfer of exogenous  $^{14}\text{C}$  between samples downstream in the  
301 reactor, labile TBM (116.35 pMC) was placed above three samples of RDC. This represents a  
302 ‘worst case’ scenario, where radiocarbon dead material is contaminated with modern carbon,  
303 and where the source of the modern contamination is completely labile in the reactor. RDC  
304 samples positioned directly below the TBM returned  $0.477$  and  $0.429 \pm 0.02$  pMC  
305 respectively (equivalent to  $42938 \pm 150$  and  $43801 \pm 167$   $^{14}\text{C}$  years, Fig 4) in duplicate runs.  
306 The radiocarbon content of the RDC samples reduces further down the profile in the reactor

307 to  $\leq 0.189 \pm 0.01$  ( $\leq 50398 \pm 252$   $^{14}\text{C}$  years) which is within error of the quartz tube  
308 background (at position 4 in Fig 2b) and below background levels after that.

309 The addition of a silica mesh spacer between the TBM and RDC samples (see fig 2c for  
310 placement), reduces the transfer of modern carbon downstream to levels that are not  
311 distinguishable from the process background. These results should be interpreted as ‘worst  
312 case’ given the very high loading of 100% labile (under HyPy conditions) and ‘modern’ (in  
313  $^{14}\text{C}$  terms) carbon that was used as the ‘contaminant’ in this case. Positioning a radiocarbon-  
314 dead sample below a significant amount of modern contaminant (~20-45mg of modern  
315 carbon), at worst, returns a value of  $<0.5$  pMC however the use of a silica mesh spacer  
316 between samples is sufficient to ensure that no subsequent samples are affected. Therefore,  
317 even when pretreating ‘worst case’ samples for radiocarbon analysis via HyPy (i.e. high  
318 levels of modern labile C that has a significantly different  $^{14}\text{C}$  age to other material analysed  
319 in the same run), these results indicate that it is acceptable to process up to 3 samples  
320 simultaneously in a 45 minute HyPy run when interspersed with silica mesh spacers.

321



322

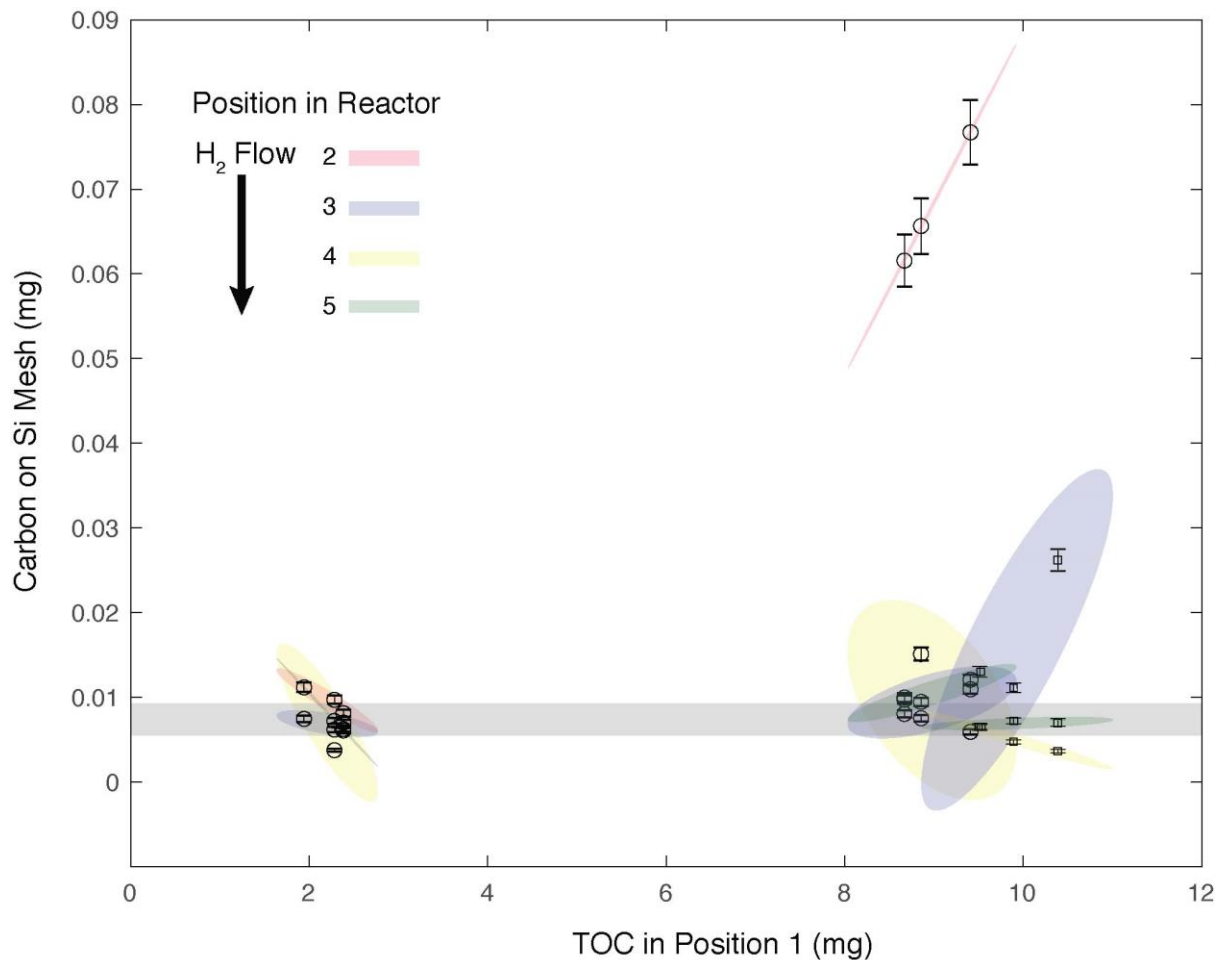
323 **Figure 4.** Radiocarbon results in pMC (without background correction) for experiment 2  
 324 indicating  $2\sigma$  error. Dashed shading indicates the accepted NERC Radiocarbon laboratory  
 325 internal quartz tube process background value of  $0.17 \pm 0.02$  pMC, grey shading indicates the  
 326 'HyPy' process background value of  $0.10 \pm 0.06$  pMC for comparison. RDC top, middle and  
 327 bottom indicates the location of the radiocarbon dead charcoal below the barley mash vessel  
 328 ( $116.35$  pMC), no silica mesh spacer was used for these samples, filled (unfilled) circles  
 329 distinguish the experiments using  $\sim 100$ mg ( $\sim 50$ mg) of barley mash.

330 3.4 Experiment 3: Assessment of downstream contamination potential by labile C

331 To quantify the amount of labile carbon transferred downstream to vessels lower in the  
 332 reactor column, a vessel containing labile carbon was placed in position 1 atop silica mesh  
 333 spacers positioned downstream (refer to fig 2d for placement). The silica mesh was analysed  
 334 for C abundance immediately following the HyPy run (see Fig 5). The silica mesh

335 background (blank) was determined to be  $0.005 \pm 0.004$  mg carbon. The high TOC  
336 experiment resulted in a transfer of  $0.07 \pm 0.02$  mg carbon (0.67% of total labile carbon) from  
337 the high organic carbon sample in position 1 onto the silica mesh directly below (at position  
338 2). The addition of an empty vessel (empty spacer) at position 2 between the high TOC  
339 sample and the silica mesh below (at position 3), reduced the transfer to  $0.02 \pm 0.02$  mg  
340 (0.09% of total labile carbon), which is an 86.6% reduction in the amount of C transfer from  
341 the sample above and within ~10% of the sample in the same position (position 3) in the  
342 previous high TOC experiment.

343 All silica mesh samples in the low TOC experiment are below the measured background  
344 (effectively 0% carbon). Silica mesh in positions 3, 4 and 5 in the high TOC experiment and  
345 positions 4 and 5 in the spacer experiment are also below background (effectively 0%  
346 carbon). In practice, it is unlikely that a 'typical' sample in a large vessel could accommodate  
347 >10mg of carbon. In this worst case scenario, there is a limited effect on the sample  
348 immediately beneath an organic-rich sample and little to no effect on the remaining samples  
349 downstream. This effect is small (i.e. <0.73% carbon is transferred from the sample above to  
350 the sample below) and can easily be addressed with the interposition of an empty spacer (or  
351 silica mesh spacer).



352

353 **Figure 5.** Milligrams of carbon transferred onto the silica mesh samples positioned below a  
 354 low TOC organic (BCM) or a high TOC organic (Sugarcane Leaves) (open circles) and a  
 355 high TOC organic material with an empty spacer at position 2 acting as a spacer (open  
 356 squares). Ellipses indicate the 95% confidence interval at each position (coloured shading).  
 357 Grey shading indicates the background silica mesh blank value of  $0.005 \pm 0.004$  mg ( $2\sigma$ ).

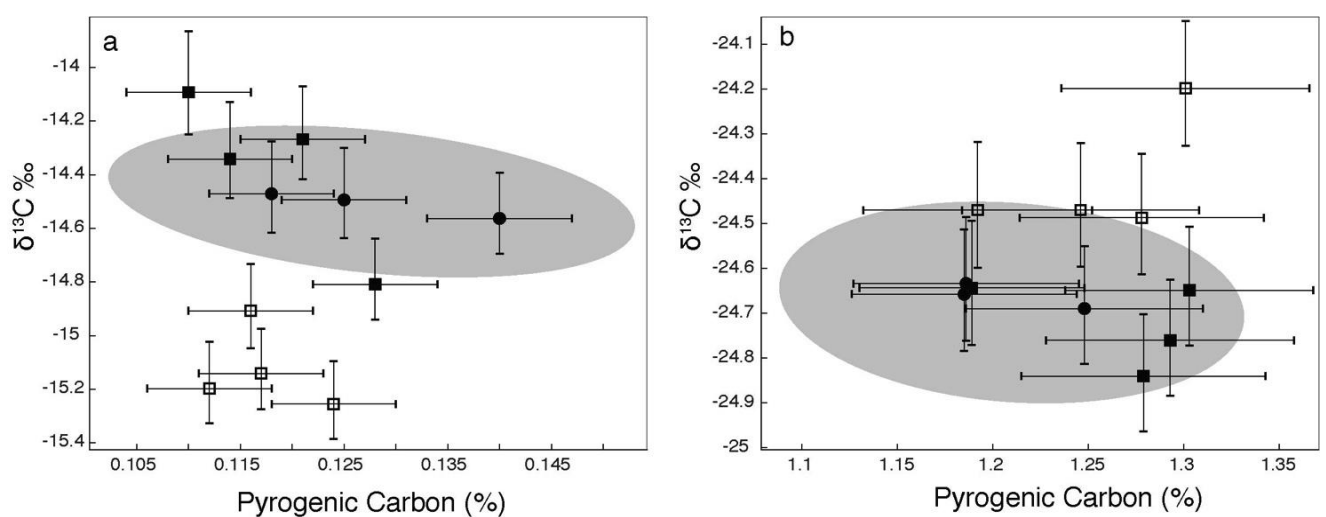
358

### 3.5 Experiment 4: Assessment of downstream contamination potential by $\delta^{13}\text{C}$

359

Isotopically dissimilar labile carbon-rich material was placed in position 1 to test whether  
 360 the  $\delta^{13}\text{C}$  value of a sample below (in position 2) is affected. The C4(C3) soils below the  
 361 C3(C4) organics in position 1, returned  $\delta^{13}\text{C}$  values which were significantly different from  
 362 the control ( $p$  value = 0.01 and 0.03 respectively), lowering (increasing) the  $\delta^{13}\text{PyC}$  of the  
 363 material below relative to the C4(C3) control (see fig 6). This effect is minimal in samples

364 with higher PyC% (fig 6b), and slightly more noticeable in samples with less PyC% (fig 6a)  
 365 resulting in an offset of 0.3‰ and 0.6‰; and 0.06% and 0.01%. The addition of an  
 366 amorphous silica mesh spacer between the two materials negates any measurable transfer of  
 367 labile carbon from the organic material above onto the soil sample below ( $t = -1.33$  and  $0.86$   
 368 respectively). In short, HyPy treatment of multiple isotopically divergent materials ( $>10\%$  in  
 369 this case) can offset  $\delta^{13}\text{PyC}$  in downstream samples by as much as 0.6‰ however, this can be  
 370 negated by the use of a silica mesh spacer.



371  
 372 **Figure 6.**  $\delta^{13}\text{PyC}$  and  $\text{PyC}(\%)$  of C4(C3) soil samples in sample vessels positioned below  
 373 C3(C4) organics a(b) in position 1. Black circles denote the C4(C3) controls, black squares  
 374 indicate that a silica mesh spacer was placed between the organic and soil sample vessels,  
 375 open squares indicate that a silica mesh spacer was not used. Grey shading indicates the  
 376 95% confidence interval of the control samples C4 soil (A) and C3 soil (B) respectively,  
 377  $\delta^{13}\text{PyC}$  and  $\text{PyC}(\%)$  error determined as per Wurster et al [31].

#### 378 4. Conclusions

379 HyPy has previously been shown to produce accurate and precise determinations of  
 380 radiocarbon abundance [12,13] and  $\delta^{13}\text{C}$  value of a well defined component of PyC [31,6].  
 381 This study has found that there is a ~7 cm zone in the HyPy reactor where reactor conditions

382 are identical and thus multiples of 7 (small) or 5 (large) samples, in bespoke borosilicate  
383 vessels, can be run in tandem within a single 45 minute HyPy run, with a precision ( $2\sigma$ ) better  
384 than 0.08% PyC and 0.6‰  $\delta^{13}\text{C}$ . Experiments using labile carbon-rich samples  
385 immediately above samples of highly divergent isotope composition were able to detect trace  
386 cross-contamination. However, radiocarbon dead PyC positioned immediately below 20-  
387 45mg of labile carbon with a high radiocarbon content resulted in  $<0.5$  pMC transfer into the  
388 radiocarbon dead sample immediately below. Similarly, small transfers were found using  
389 samples widely divergent in  $\delta^{13}\text{C}$  value. Cross-contamination only occurred in the sample  
390 immediately below the labile carbon source and did not carry downstream to samples lower  
391 in the reactor. In all cases, the use of a silica mesh spacer eliminated cross-contamination  
392 between samples. Therefore, even when pretreating ‘dirty’ samples for radiocarbon or stable  
393 isotope analysis using HyPy, the results indicate that it is acceptable to process up to 3  
394 samples simultaneously. In addition, lower radiocarbon backgrounds were obtained using the  
395 HyPy process in comparison to standard pretreatment protocols at NCRF, suggesting further  
396 potential for application as a low blank pretreatment for radiocarbon dating should be further  
397 investigated.

398 The step that currently limits the application of hydrogen pyrolysis for PyC isolation and  
399 analysis is the 43 minute temperature ramp to remove labile carbon (and subsequent 23  
400 minute period required for cooling), with only  $\sim 7$  samples able to be processed in a single  
401 day. This study suggests that 3 (with spacers) to 7 (without spacers) samples can be processed  
402 in a single run without diminishing accuracy or precision, enabling  $\sim 20$ -50 samples to be  
403 processed in a day. This is comparable to the number of samples that can be run by EA-IRMS  
404 for stable isotopes in a day, removing the current bottleneck in routine application to larger  
405 scale projects where quantification of PyC and determination of isotope composition is  
406 required.

407 **Acknowledgements**

408 This research was funded by the Australian Research Council Centre of Excellence  
409 for Australian Biodiversity and Heritage (CE170100015) and an Australian Research Council  
410 Laureate Fellowship to M.I.B (FL140100044).

411 **References**

- 412 1 Bird MI, Wynn JG, Saiz G, Wurster CM, McBeath A. The Pyrogenic Carbon Cycle.  
413 *Annual Review of Earth and Planetary Sciences*. 2015;43(1):273-298.  
414 doi:10.1146/annurev-earth-060614-105038.  
415
- 416 2 Santin C, Doerr SH, Kane ES, Masiello CA, Ohlson M, de la Rosa JM, Preston CM,  
417 Dittmar T. Towards a global assessment of pyrogenic carbon from vegetation fires.  
418 *Glob Chang Biol*. 2016;22(1):76-91. doi:10.1111/gcb.12985.  
419
- 420 3 Reisser M, Purves RS, Schmidt MWI, Abiven S. Pyrogenic Carbon in Soils: A  
421 Literature-Based Inventory and a Global Estimation of Its Content in Soil Organic  
422 Carbon and Stocks. *Frontiers in Earth Science*. 2016;4doi:10.3389/feart.2016.00080.  
423
- 424 4 Koele N, Bird M, Haig J, Marimon BH, Marimon BS, Phillips OL, de Oliveira EA,  
425 Quesada CA, Feldpausch TR. Amazon Basin forest pyrogenic carbon stocks: First  
426 estimate of deep storage. *Geoderma*. 2017;306:237-243.  
427 doi:10.1016/j.geoderma.2017.07.029.  
428
- 429 5 Sohi SP, Krull E, Lopez-Capel E, Bol R. Chapter 2 - A Review of Biochar and Its Use  
430 and Function in Soil. In: Sparks, D. L. ed. *Advances in Agronomy*. Elsevier; 2010:47-  
431 82.  
432
- 433 6 Wurster CM, McBeath AV, Bird MI. The carbon isotope composition of semi-labile  
434 and stable pyrogenic carbon in a thermosequence of C3 and C4 derived char. *Organic*  
435 *Geochemistry*. 2015;81:20-26. doi:10.1016/j.orggeochem.2015.01.008.  
436
- 437 7 Hammes K, Schmidt MWI, Smernik RJ, Currie LA, Ball WP, Nguyen TH,  
438 Louchouart P, Houel S, Gustafsson O, Elmquist M, Cornelissen G, Skjemstad JO,  
439 Masiello CA, Song J, Peng P, Mitra S, Dunn JC, Hatcher PG, Hockaday WC, Smith  
440 DM, Hartkopf-Froeder C, Boehmer A, Luer B, Huebert BJ, Amelung W, Brodowski  
441 S, Huang L, Zhang W, Gschwend PM, Flores-Cervantes DX, Largeau C, Rouzaud  
442 JN, Rumpel C, Guggenberger G, Kaiser K, Rodionov A, Gonzalez-Vila FJ, Gonzalez-  
443 Perez JA, de la Rosa JM, Manning DAC, Lopez-Capel E, Ding L. Comparison of  
444 quantification methods to measure fire-derived (black/elemental) carbon in soils and  
445 sediments using reference materials from soil, water, sediment and the atmosphere.  
446 *Global Biogeochemical Cycles*. 2007;21(3)doi:10.1029/2006gb002914.  
447
- 448 8 Knicker H, Almendros G, González-Vila FJ, Martín F, Lüdemann HD. 13C- and  
449 15N-NMR spectroscopic examination of the transformation of organic nitrogen in

- 450 plant biomass during thermal treatment. *Soil Biology and Biochemistry*.  
451 1996;28(8):1053-1060. doi:10.1016/0038-0717(96)00078-8.  
452
- 453 9 Chang Z, Tian L, Li F, Zhou Y, Wu M, Steinberg CEW, Dong X, Pan B, Xing B.  
454 Benzene polycarboxylic acid - A useful marker for condensed organic matter, but not  
455 for only pyrogenic black carbon. *Sci Total Environ*. 2018;626:660-667.  
456 doi:10.1016/j.scitotenv.2018.01.145.  
457
- 458 10 Love GD, Snape CE, Carr AD, Houghton RC. Release of covalently-bound alkane  
459 biomarkers in high yields from kerogen via catalytic hydrolysis. *Organic*  
460 *Geochemistry*. 1995;23(10):981-986. doi:10.1016/0146-6380(95)00075-5.  
461
- 462 11 Craig OE, Love GD, Isaksson S, Taylor G, Snape CE. Stable carbon isotopic  
463 characterisation of free and bound lipid constituents of archaeological ceramic vessels  
464 released by solvent extraction, alkaline hydrolysis and catalytic hydrolysis.  
465 *Journal of Analytical and Applied Pyrolysis*. 2004;71(2):613-634.  
466 doi:10.1016/j.jaap.2003.09.001.  
467
- 468 12 Ascough PL, Bird MI, Brock F, Higham TFG, Meredith W, Snape CE, Vane CH.  
469 Hydrolysis as a new tool for radiocarbon pre-treatment and the quantification of  
470 black carbon. *Quaternary Geochronology*. 2009;4(2):140-147.  
471 doi:10.1016/j.quageo.2008.11.001.  
472
- 473 13 Ascough PL, Bird MI, Meredith W, Wood RE, Snape CE, Brock F, Higham TFG,  
474 Large DJ, Apperley DC. Hydrolysis: Implications for Radiocarbon Pretreatment  
475 and Characterization of Black Carbon. *Radiocarbon*. 2010;52(3):1336-1350.  
476 doi:10.1017/S0033822200046427.  
477
- 478 14 Meredith W, Ascough PL, Bird MI, Large DJ, Snape CE, Sun Y, Tilston EL.  
479 Assessment of hydrolysis as a method for the quantification of black carbon  
480 using standard reference materials. *Geochimica Et Cosmochimica Acta*. 2012;97:131-  
481 147. doi:10.1016/j.gca.2012.08.037.  
482
- 483 15 Robert AM, Grotheer H, Greenwood PF, McCuaig TC, Bourdet J, Grice K. The  
484 hydrolysis (HyPy) release of hydrocarbon products from a high maturity kerogen  
485 associated with an orogenic Au deposit and their relationship to the mineral matrix.  
486 *Chemical Geology*. 2016;425:127-144. doi:10.1016/j.chemgeo.2016.01.028.  
487
- 488 16 Rombola AG, Fabbri D, Meredith W, Snape CE, Dieguez-Alonso A. Molecular  
489 characterization of the thermally labile fraction of biochar by hydrolysis and  
490 pyrolysis-GC/MS. *Journal of Analytical and Applied Pyrolysis*. 2016;121:230-239.  
491 doi:10.1016/j.jaap.2016.08.003.  
492
- 493 17 Sephton MA, Love GD, Meredith W, Snape CE, Sun CG, Watson JS.  
494 Hydrolysis: A new technique for the analysis of macromolecular material in  
495 meteorites. *Planetary and Space Science*. 2005;53(12):1280-1286.  
496 doi:10.1016/j.pss.2005.06.008.  
497

- 498 18 Foereid B, Lehmann J, Wurster C, Bird M. Presence of Black Carbon in Soil due to  
499 Forest Fire in the New Jersey Pine Barrens. *Journal of Earth Science and*  
500 *Engineering*. 2015;5(2):91-97. doi:10.17265/2159-581x/2015.02.001.  
501
- 502 19 Santin C, Doerr SH, Merino A, Bucheli TD, Bryant R, Ascough P, Gao X, Masiello  
503 CA. Carbon sequestration potential and physicochemical properties differ between  
504 wildfire charcoals and slow-pyrolysis biochars. *Sci Rep*. 2017;7(1):11233.  
505 doi:10.1038/s41598-017-10455-2.  
506
- 507 20 Wurster CM, Saiz G, Schneider MPW, Schmidt MWI, Bird MI. Quantifying  
508 pyrogenic carbon from thermosequences of wood and grass using hydrogen pyrolysis.  
509 *Organic Geochemistry*. 2013;62:28-32. doi:10.1016/j.orggeochem.2013.06.009.  
510
- 511 21 Meredith W, McBeath A, Ascough P, Bird MI. Analysis of biochars by  
512 hydrolysis (HyPy). In: Singh, B., Camps Arbestain, M. & Lehmann, J. eds.  
513 *Biochar: A Guide to Analytical Methods*. Clayton: CRC Press; 2017.  
514
- 515 22 Grotheer H, Greenwood PF, McCulloch MT, Böttcher ME, Grice K.  $\delta^{34}\text{S}$  character  
516 of organosulfur compounds in kerogen and bitumen fractions of sedimentary rocks.  
517 *Organic Geochemistry*. 2017;110:60-64. doi:10.1016/j.orggeochem.2017.04.005.  
518
- 519 23 Saiz G, Goodrick I, Wurster C, Nelson PN, Wynn J, Bird M. Preferential Production  
520 and Transport of Grass-Derived Pyrogenic Carbon in NE-Australian Savanna  
521 Ecosystems. *Frontiers in Earth Science*. 2018;5(1):115.  
522 doi:10.3389/feart.2017.00115.  
523
- 524 24 Field E, Marx S, Haig J, May JH, Jacobsen G, Zawadzki A, Child D, Heijnis H,  
525 Hotchkis M, McGowan H, Moss P. Untangling geochronological complexity in  
526 organic spring deposits using multiple dating methods. *Quaternary Geochronology*.  
527 2018;43:50-71. doi:10.1016/j.quageo.2017.10.002.  
528
- 529 25 Zhang XY, Huang DS, Deng H, Snape C, Meredith W, Zhao Y, Du Y, Chen X, Sun  
530 YG. Radiocarbon dating of charcoal from the Bianjiashan site in Hangzhou: New  
531 evidence for the lower age limit of the Liangzhu Culture. *Quaternary Geochronology*.  
532 2015;30:9-17. doi:10.1016/j.quageo.2015.07.001.  
533
- 534 26 Llorente M, Turrion MB, Glaser B. Rapid and economical quantification of black  
535 carbon in soils using a modified benzene polycarboxylic acids (BPCA) method.  
536 *Organic Geochemistry*. 2018;115:197-204. doi:10.1016/j.orggeochem.2017.11.005.  
537
- 538 27 Gulliksen S, Scott M. Report of the TIRI workshop, Saturday 13 August 1994.  
539 *Radiocarbon*. 1995;37(2):820-821. doi:10.1017/S0033822200031404.  
540
- 541 28 Rozanski K, Stichler W, Gonfiantini R, Scott EM, Beukens RP, Kromer B, Van Der  
542 Plicht J. The IAEA 14C Intercomparison Exercise 1990. *Radiocarbon*.  
543 2016;34(3):506-519. doi:10.1017/s0033822200063761.  
544
- 545 29 Bird MI, Levchenko V, Ascough PL, Meredith W, Wurster CM, Williams A, Tilston  
546 EL, Snape CE, Apperley DC. The efficiency of charcoal decontamination for

547 radiocarbon dating by three pre-treatments - ABOX, ABA and hypy. *Quaternary*  
548 *Geochronology*. 2014;22:25-32. doi:10.1016/j.quageo.2014.02.003.  
549

550 30 Love GD, McAulay A, Snape CE, Bishop AN. Effect of process variables in catalytic  
551 hydrolysis on the release of covalently bound aliphatic hydrocarbons from  
552 sedimentary organic matter. *Energy & Fuels*. 1997;11(3):522-531.  
553 doi:10.1021/ef960194x.  
554

555 31 Wurster CM, Lloyd J, Goodrick I, Saiz G, Bird MI. Quantifying the abundance and  
556 stable isotope composition of pyrogenic carbon using hydrogen pyrolysis. *Rapid*  
557 *Commun Mass Spectrom*. 2012;26(23):2690-2696. doi:10.1002/rcm.6397.  
558

559 32 Slota PJ, Jull AJT, Linick TW, Toolin LJ. Preparation of Small Samples for <sup>14</sup>C  
560 Accelerator Targets by Catalytic Reduction of CO. *Radiocarbon*. 1987;29(2):303-  
561 306. doi:10.1017/s0033822200056988.  
562

563 33 Stuiver M, Polach HA. Discussion Reporting of <sup>14</sup>C Data. *Radiocarbon*.  
564 2016;19(3):355-363. doi:10.1017/s0033822200003672.  
565  
566

567  
568  
569  
570  
571  
572  
573  
574  
575  
576  
577  
578  
579

580 **Table 1.** *Consensus values for in-house materials used in experiments to assess variation in*  
 581 *measured PyC abundance and  $\delta^{13}\text{C}$  value when combining multiple samples during a single*  
 582 *hydropyrolysis run (error is reported as  $2\sigma$ ).*

| Soil Samples           |                   | TOC (%)         | $\delta^{13}\text{C}$ | PyC (%)         | $\delta^{13}\text{PyC}$ |
|------------------------|-------------------|-----------------|-----------------------|-----------------|-------------------------|
|                        | BC Mollisol (BCM) | 2.04 $\pm$ 0.02 | -25.57 $\pm$ 0.2      | 0.25 $\pm$ 0.1  | -26.47 $\pm$ 0.6        |
| C3                     | SAN2 Surface      | 13.44 $\pm$ 0.6 | -25.73 $\pm$ 0.5      | 1.18 $\pm$ 0.1  | -24.66 $\pm$ 0.2        |
| C4                     | AGR               | 1.51 $\pm$ 0.1  | -16.51 $\pm$ 0.1      | 0.15 $\pm$ 0.01 | -14.74 $\pm$ 0.3        |
| Labile Organic Samples |                   |                 |                       |                 |                         |
| C3                     | Rainforest Leaves | 44.08 $\pm$ 4.4 | -33.47 $\pm$ 0.1      | N/A             | N/A                     |
| C4                     | Sugarcane Leaves  | 42.11 $\pm$ 4.2 | -11.86 $\pm$ 0.3      | N/A             | N/A                     |

583

584

585

586

587

588

589

590

591

592

593

594 **Table 2.** *Position experiment summary statistics*

| BCM | Position | PyC (%) |           | $\delta^{13}\text{PyC}$ (‰) |           |
|-----|----------|---------|-----------|-----------------------------|-----------|
|     |          | $\mu$   | $2\sigma$ | $\mu$                       | $2\sigma$ |
|     | 1        | 0.3     | 0.04      | -26.2                       | 0.3       |
|     | 2        | 0.3     | 0.12      | -26.2                       | 0.4       |
|     | 3        | 0.2     | 0.02      | -26.6                       | 0.4       |
|     | 4        | 0.2     | 0.04      | -26.7                       | 0.3       |
|     | 5        | 0.2     | 0.04      | -26.7                       | 0.2       |
|     | 6        | 0.2     | 0.08      | -26.4                       | 0.9       |
|     | 7        | 0.3     | 0.08      | -26.7                       | 0.2       |
|     | 8        | 0.5     | 0.18      | -26.5                       | 0.3       |
|     | 9        | 0.9     | 0.36      | -26.2                       | 1         |
| AGR | 1        | 0.2     | 0.01      | -14.8                       | 0.4       |
|     | 2        | 0.2     | 0.01      | -14.7                       | 0.2       |
|     | 3        | 0.1     | 0.03      | -14.6                       | 0.5       |
|     | 4        | 0.2     | 0.04      | -14.7                       | 0.4       |
|     | 5        | 0.1     | 0.02      | -14.9                       | 0.1       |
|     | 6        | 0.2     | 0.07      | -15.3                       | 0.8       |

595

596